Steel and Composite Structures, *Vol. 34, No. 2 (2020) 261-277*
DOI: https://doi.org/10.12989/scs.2020.34.2.261

Influence of vacancy defects on vibration analysis of graphene sheets applying isogeometric method: Molecular and continuum approaches

Vahid Tahouneh*, Mohammad Hasan Naei and Mahmoud Mosavi Mashhadi

School of Mechanical Engineering, College of Engineering, University of Tehran, Tehran, Iran

(*Received August 2, 2019, Revised November 29, 2019, Accepted December 2, 2019*)

Abstract. The main objective of this research paper is to consider vibration analysis of vacancy defected graphene sheet as a nonisotropic structure via molecular dynamic and continuum approaches. The influence of structural defects on the vibration of graphene sheets is considered by applying the mechanical properties of defected graphene sheets. Molecular dynamic simulations have been performed to estimate the mechanical properties of graphene as a nonisotropic structure with single- and double- vacancy defects using open source well-known software i.e., large-scale atomic/molecular massively parallel simulator (LAMMPS). The interactions between the carbon atoms are modelled using Adaptive Intermolecular Reactive Empirical Bond Order (AIREBO) potential. An isogeometric analysis (IGA) based upon non-uniform rational B-spline (NURBS) is employed for approximation of single-layered graphene sheets deflection field and the governing equations are derived using nonlocal elasticity theory. The dependence of small-scale effects, chirality and different defect types on vibrational characteristic of graphene sheets is investigated in this comprehensive research work. In addition, numerical results are validated and compared with those achieved using other analysis, where an excellent agreement is found. The interesting results indicate that increasing the number of missing atoms can lead to decrease the natural frequencies of graphene sheets. It is seen that the degree of the detrimental effects differ with defect type. The Young's and shear modulus of the graphene with SV defects are much smaller than graphene with DV defects. It is also observed that Single Vacancy (SV) clusters cause more reduction in the natural frequencies of SLGS than Double Vacancy (DV) clusters. The effectiveness and the accuracy of the present IGA approach have been demonstrated and it is shown that the IGA is efficient, robust and accurate in terms of nanoplate problems.

Keywords: defected graphene; vibration analysis; isogeometric method; NURBS; nonlocal elasticity theory; molecular dynamic

1. Introduction

Indubitable, one of the most significant allotropes of carbon is graphene containing a single layer of carbon atoms organized in a honeycomb-like pattern. Due to the having extraordinary properties such as lightness and strength, graphene can be abundantly applied in engineering structures such as aerospace structure (Kuzhir *et al.* 2013), bio-structures (Ali *et al.* 2017). On the other hand, Graphene sheets (GSs) are the two dimensional structures containing unbeatable lattice structures, supreme electronic and mechanical characteristics. So far, a number of techniques have been extended to attain GSs including Hummer method and exfoliation (Marina *et al*. 2016, Ali *et al*. 2015), exfoliation of graphite in solvents, micromechanical exfoliation (Al-Sherbini *et al.* 2017, Tasis *et al*. 2013, Siddique *et al.* 2015). Until today, many investigation projects have been conducted to investigate the mechanical behaviors of the single-layered graphene sheet (SLGS) such as free and forced vibration (Sakhaee-Pour *et al.* 2008, Song *et al.* 2017), buckling (Sakhaee-Pour 2009, Rouhi and Ansari 2012), and bending (Sobhy 2014, Wei *et al.* 2012) behaviors. A hybrid atomistic-structural element proposed by Sadeghi and Naghdabadi (2010) to investigate the infinitesimal and large amplitude of SLGS.

Today, a life without nanotechnology is hard to imagine. Utilizing nanotechnology, materials can effectively be made stronger, lighter, more durable, more reactive, more sieve-like, or better electrical conductors, among many other traits.

Considering the importance of investigating the behavior of nanostructures, some researchers utilized empirical testing and atomistic simulation results (Chen *et al.* 2006, Stan *et al.* 2007) to demonstrate this theorem that by reducing the material size to the micro/nano scale, the effect of size-dependent materials becomes remarkable. Formerly, the weakness of the classical continuum theories to capture the size effect has been proved by researchers. Hence, certain higher-order continuum theories containing the independent internal length scale parameter have been developed (Eringen 1983, Lam *et al*. 2003, Yang *et al.* 2002, Lim *et al.* 2015). One of these non-traditional theories is called nonlocal elasticity theory proposed by Eringen (1983) including a material length scale term to predict the size effect. Because of modelling carbon nanotubes and fullerenes as GSs in applications, studying the behavior of GSs in micro/nano scale is a significant subject. By taking into account nonlocal elasticity theory in conjunction with

*Corresponding author, Ph.D. Student
E-mail: vahid.tahouneh@ut.ac.ir

Copyright © 2020 Techno-Press, Ltd.

ISSN: 1229-9367 (Print), 1598-6233 (Online)

the first-order shear deformation theory (FSDT), Ansari *et al.* (2010) investigated the resonant frequencies of SLGS under various boundary conditions using generalized differential quadrature method (GDQM). The authors employed the molecular dynamics (MD) approach for estimating the suitable values of nonlocal parameter. Pradhan and Kumar (2010) studied the natural frequencies of orthotropic SLGS via nonlocal differential constitutive relations of Eringen (1983). Applying the kp-Ritz method with the nonlocal continuum assumption, Zhang *et al.* (2015) analyzed the free vibration of SLGS. Based on the nonlinear von Kármán terms and nonlocal elasticity theory, Ribeiro and Chuaqui (2019) examined the nonlinear modes of vibration of SLGS using Airy stress function. Kumar and Srivastava (2016) studied Elastic properties of CNT- and Graphene-reinforced nanocomposites using RVE. Hosseini and Zhang (2018) considered transient dynamic analysis and elastic wave propagation in a functionally graded graphene platelets (FGGPLs)-reinforced composite thick hollow cylinder, which is subjected to shock loading. Moradi-Dastjerdi and Behdinan (2019) studied thermoelastic static and free vibrational behaviors of axisymmetric thick cylinders reinforced with functionally graded (FG) randomly oriented graphene subjected to internal pressure and thermal gradient loads. Javani et al. (2019) studied buckling analyses of composite plate reinforced by Graphen platelate (GPL). Karami *et al.* (2018) used three-dimensional (3D) elasticity theory in conjunction with nonlocal strain gradient theory (NSGT) to develop for mechanical analysis of anisotropic nanoparticles. Ahmed Houari et ql. (2018) presented a closed-form solutions for exact critical buckling loads of nonlocal strain gradient functionally graded beams. Shahsavari *et al.* (2018) developed a high-order nonlocal strain gradient model for wave propagation analysis of porous FG nanoplates resting on a gradient hybrid foundation in thermal environment. Karami *et al.* (2017) investigated the influences of triaxial magnetic field on the wave propagation behavior of anisotropic nanoplates. Karami *et al.* (2018) used a new size-dependent quasi-3D plate theory for wave dispersion analysis of functionally graded nanoplates while resting on an elastic foundation and under the hygrothermal environment. Marin (2008) proved the existence and uniqueness of the generalized solutions for the boundary value problems in elasticity of initially stressed bodies with voids (porous materials). Marin and Baleanu (2016) dedicated to the spatial behavior of the harmonic in time vibrations within the model of the linear thermoelasticity theory without dissipation energy for micropolar bodies. Marin (2016) formulated a heat-flux theory for taking into account a new set of state variables including the heat-flux vector and an evolution equation for it. Tornabene *et al.* (2018) studied free vibration of laminated nanocomposite plates and shells using first-order shear deformation theory and the Generalized Differential Quadrature (GDQ) method. Each layer of the laminate was modelled as a three-phase composite. A survey of several methods under the heading of strong formulation finite element method (SFEM) was presented by Tornabene *et al.* (2015). These approaches were distinguished from classical one, termed weak formulation finite element method (WFEM). Isogeometric approach, an efficient and useful numerical method, has been introduced by Hughes *et al.* (2005) which fulfills a gap between computer aided design (CAD) and finite element analysis (FEA). Main ideas of this method are to adopt the CAD basis functions (e.g., the NURBS) to the shape functions in the finite element analysis. Bilotta *et al.* (2010) proposed a three-dimensional finite element, named HC3, based on a quadratic B-spline interpolation of the displacement field for the linear elastic analysis of three-dimensional problems. This proposed element was an extension of the high-continuity (HC) finite element presented by Aristodemo (1985) for two-dimensional elasticity which is the first investigation on the HC finite element. The accuracy and efficiency of the isogeometric analysis for structures such as beams and plates have been demonstrated by a number of works in these years, e.g., (Guo *et al*. 2014, Kapoor and Kapania 2012, Le-Manh and Lee 2014, Le-Manh *et al.* 2016, Malagu *et al.* 2012, Thai *et al.* 2012, Tran *et al.* 2015, 2016, Wang *et al*. 2015, Yu *et al.* 2015). Soleimani *et al.* (2017) investigated the critical buckling loads of GSs under various values of nonlocal parameters and different boundary conditions using IGA based on NURBS. Also, IGA is taken into account to analyze the thermal buckling problem of composite laminated plates reinforced with GSs by Mirzaei and Kiani (2017). A variety of theoretical methods have been used to examine the mechanical and elastic properties of an ideal and flawless single-layer graphene sheet, including density functional theory (DFT), quantum mechanics, molecular dynamic simulation and continuous medium mechanics. Liu *et al*. (2007) found Young's modulus as 1.05 TPa for single-layer graphene using the density functional technique. Jiang *et al*. (2009) investigated Young's modulus for different sizes of single-layer graphene at different temperatures using molecular dynamics. Shen *et al*. (2010) examined Young's and shear moduli of nanoscale structures at different temperatures. The analysis of failure and ultimate strength of single-layer graphene sheets was carried out by Ni *et al.* (2010), who showed that these nanostructures are much stronger in armchair alignment than zigzag alignment. Tsai and Tu (2010) examined the mechanical properties of graphene by molecular dynamics. The main problems with atomic models include time-consuming calculations and the subsequent limitation in the dimensions of molecular and atomic structures. Great efforts have therefore been made in recent years to develop nanoscale theories of continuous medium mechanics. To this end, Reddy *et al.* (2006) found Young's modulus as 0.669 TPa for single-layer graphene using continuous medium mechanics. Sakhaee-Pour (2009) and Georgantzinos *et al.* (2010) found Young's modulus values as 1.025 TPa and 1.367 TPa respectively, using the finite element technique, in which the atomic bonds were modelled as truss, beam or spring.

Due to the fact that during the production process and under constrains conditions, it is possible SLGS may be defected (Compagnini *et al.* 2009, Martinez-Asencio and Caturla 2015, Sun *et al*. 2013, Rajasekaran *et al*. 2016), therefore, it is critical to study the influence of these structural defects such as vacancies on the mechanical

characteristics of SLGS. On the other hand, cut-outs or vacancies may be made to lighten the structure or to alter the resonant frequencies of SLGS. Graphene sheets appear as wrinkled when in equilibrium. These wrinkles can have a height of 7 Å. Moreover, defects called the ridge defect also appear on graphene sheets due to shearing strain (Udupa and Martini 2011). Bu *et al*. (2009) used molecular dynamic simulation to assess the mechanical properties of armchair-structured graphene nanoribbons at 300 K. This simulation indicated the presence of 0.88-nm-high bulges and wrinkles in the nanoribbons equivalent to approximately a 5%-strain on the nanoribbon. Kvashnin *et al*. (2010) investigated the properties of circular graphene for various radii and also the effect of different densities of vacancy defects on the mechanical properties of single-layer graphene sheet. The Stone-Wales defect in graphene and other substances with a covalence bond configuration of the geometric type sp^2 were investigated by Ma *et al.* (2009). Tahouneh *et al.* (2018) investigated the effects of site and size of vacancy defects on the mechanical properties of graphene as an anisotropic structure using the lekhnitskii interaction coefficients and Molecular Dynamic approach. Jalali *et al*. (2016) investigated the influence of out-of-plane defects on vibrational analysis of single layered graphene sheets. Zhang *et al.* (2009) used the governing equations and simulation to indicate that the gas-identification property of chemical sensors increases significantly in graphene with the vacancy defect compared to defect-free graphene. Sun *et al.* (2014) also studied the effect of vacancy defects on the ultimate strength of graphene sheets. In another study (Sun *et al*. 2015), molecular dynamic modelling was used to investigate the effect of defects on the unique properties of graphene while considering graphene an anisotropic structure. This research work revealed that graphene properties are totally dependent on angular orientation. The authors showed that the mechanical properties of graphene sheets are least sensitive to vacancy defects at the angle of 15 degree. Wu *et al*. (2015) found dynamic properties and relaxation time for a variety of graphene groups with vacancy defects using molecular dynamic simulation in Large-scale Atomic/Molecular Massively Parallel Simulator (LAMMPS). They showed that the maximum dynamic displacements of graphene increase with the number and size of vacancy defects. Based on theories relating to graphene molecular bonds, Xie *et al.* (2014) studied the effect of single- and double-vacancy defects on the photonic properties and thermal conductivity of graphene with defects and showed that the type of these defects has a significant effect on the photo and thermal conductivity of graphene. Neek-Amal and Peeters (2010) performed the MD simulation of nano-indentation of circular graphene sheets similar to the experiments of Lee *et al.* (2008). Utilizing quantum mechanics, Yanovsky *et al.* (2009) obtained mechanical properties of graphene sheets. Soleimani *et al.* (2019) investigated the effects of inevitable out-of-plane defects on the postbuckling behavior of single-layered graphene sheets (SLGSs) under in-plane loadings based on nonlocal first order shear deformation theory. According to the nonlocal continuum assumption, the effect of defect modeled as eccentric hole on the elastic instability of an annular SLGS resting on elastic medium is analytically reported by Fadaee (2016) applying translational addition theorem. Dastjerdi *et al.* (2016) developed a nonlocal model based upon FSDT to analyze the bending problem of annular SLGS under with an eccentric vacant defect. The authors demonstrated that the influence of attendance of vacancy defect is extremely depends on the kinds of boundary conditions. Mirakhory *et al*. (2018) obtained the natural frequencies of the defected triangular GSs and reported that the defective equilateral triangular GSs have the highest values of resonance. Employing the Monte Carlo simulation based finite element method, Chu *et al*. (2018) investigated the natural frequencies of vacancy defected GSs. They indicated that an increase in the value of thickness and Young's modulus of GSs leads to smaller values of natural frequencies.

Despite the aforementioned extensive research on the vibration analysis of graphene sheets using nonlocal elasticity theory, to the authors' best knowledge, still very little work has been done for vibration analysis of defected graphenes as a nonisotropic structure via molecular dynamic and continuum approaches. The aim of this study is to fill this apparent gap in this area by investigating the effects of vacancies on vibrational characteristic of SLGS.

2. Isogeometric formulation for vibration analysis

2.1 NURBS basis functions

A brief fundamental of some technical features of B-spline and NURBS basis functions for isogeometric analysis is presented. A detailed description of the NURBS, one may reach, e.g., see Piegl and Tiller (1997). A NURBS curve $\mathbf{X}(\xi)$ of order p is defined as

$$X(\xi)=\sum_{i=1}^{n} R_{i,p}(\xi)\tilde{X}_i, \tag{1}$$

$$R_{i,p}(\xi)=\frac{N_{i,p}(\xi)\omega_i}{\sum_{j=1}^{n} N_{j,p}(\xi)\omega_j}, \tag{2}$$

where $R_{i,p}$ stands for the univariate NURBS basis functions, $\tilde{X}_i = (x_i, y_i)$; i =1, 2, . . . , n are a set of *n* control points, *wi* are a set of *n* weights corresponding to the control points that must be non-negative and $N_{i,p}$ represents the B-spline basis function of order p. To construct a set of n B-spline basis functions of order p, a knot vector Ξ is defined in a parametric space as

$$\Xi=\left\{\xi_1,\xi_2,...,\xi_{n+p+1}\right\} \quad \xi_i \le \xi_{i+1}, \quad i=1,2,...,n+p \tag{3}$$

The parametric space is assumed to be $\xi \in [0, 1]$. The knot vectors used for analysis purposes are generally open knot vectors to satisfy the Kronecker-delta property at boundary points (Roh and Cho 2004). The knot vector is said to be open if the knots are repeated *p*+1 times at the start and end of the vector. Given a knot vector, the univariate B-spline basis function $N_{i,p}$ can be constructed by the following Cox-de Boor recursion formula (Piegl and Tiller 1997)

$$N_{i,0}(\xi)=\begin{cases}1 & \text{if} \quad \xi_i \le \xi \le \xi_{i+1}\\ 0 & \text{otherwise}\end{cases} \tag{4}$$

and

$$N_{i,p}(\xi)=\frac{\xi-\xi_i}{\xi_{i+p}-\xi_i}N_{i,p-1}(\xi)+\frac{\xi_{i+p+1}-\xi}{\xi_{i+p+1}-\xi_{i+1}}N_{i+1,p-1}(\xi), \tag{5}$$
$$p=1,2,3,...$$

The B-spline functions which are constructed from the open knot vectors have the interpolation feature at the ends of the parametric space. A cubic B-spline basis functions with the interpolation feature at the ends of the parametric space are shown in Fig. 1.

Generally, a NURBS surface of order p in ξ direction and order q in η direction can be expressed as

$$X(\xi,\eta)=\sum_{i=1}^{n}\sum_{j=1}^{m}R_{i,j}^{p,q}(\xi,\eta)\tilde{X}_{i,j}$$
$$=\sum_{i=1}^{n}\sum_{j=1}^{m}\frac{N_{i,p}(\xi)M_{j,q}(\eta)\omega_{i,j}}{\sum_{\hat{i}}^{n}\sum_{\hat{j}}^{m}N_{\hat{i},p}(\xi)M_{\hat{j},q}(\eta)\omega_{\hat{i},\hat{j}}}\tilde{X}_{i,j},0\le\xi,\eta\le1 \tag{6}$$

where $R_{i,j}^{p,q}$ stands for the bivariate NURBS basis functions, $\tilde{X}_{i,j}$ is a control mesh of n×m control points, and $\omega_{i,j}$ are the corresponding weights, while $N_{i,p}$ and $M_{j,q}$ are the B-spline basis functions defined on the Ξ and H knot vectors, respectively. The first derivative of $R_{i,j}^{p,q}(\xi,\eta)$ with respect to each parametric variable, e.g., ξ, is derived by simply applying the quotient rule to Eq. (6) as

$$\frac{\partial R_{i,j}^{p,q}(\xi,\eta)}{\partial\xi}=$$
$$\frac{\frac{\partial N_{i,p}(\xi)}{\partial\xi}M_{j,q}(\eta)\omega_{i,j}W(\xi,\eta)-\frac{\partial W(\xi,\eta)}{\partial\xi}N_{i,p}(\xi)M_{j,q}(\eta)\omega_{i,j}}{(W(\xi,\eta))^2} \tag{7}$$

and

$$W(\xi,\eta)=\sum_{\hat{i}}^{n}\sum_{\hat{j}}^{m}N_{\hat{i},p}(\xi)M_{\hat{j},q}(\eta)\omega_{\hat{i},\hat{j}} \tag{8}$$

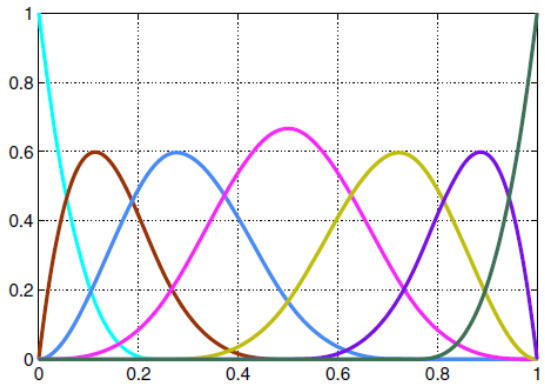

Fig. 1 Cubic basis functions for an open knot vector Ξ={0,0,0,0,0.25,0.5,0.75,1,1,1,1}

$$\frac{\partial W(\xi,\eta)}{\partial\xi}=\sum_{\hat{i}}^{n}\sum_{\hat{j}}^{m}\frac{\partial N_{\hat{i},p}(\xi)}{\partial\xi}M_{\hat{j},q}(\eta)\omega_{\hat{i},\hat{j}} \tag{9}$$

To earn more detail about the NURBS and its characteristics, the reader is referred to Ref. (Piegl and Tiller 1997). It is worthwhile to note that in the IGA analysis, by using the isoparametric concept, the NURBS basis is employed for both the parametrization of the geometry and the approximation of the solution field, which is the plate deflection w(x) in this paper, as follows

$$w^h(x(\xi))=\sum_{I=1}^{n\times m}\phi_I(\xi)w_I \tag{10}$$

$$x(\xi)=\sum_{I=1}^{n\times m}\phi_I(\xi)\tilde{x}_I \tag{11}$$

In all the above equations, ξ=(ξ,η) is the parametric coordinates, **x**=(*x*,*y*) is the physical coordinates, $\tilde{x}_I$ represents the control points of a n×m control mesh, w_I represents the deflection of the plate at each control point, and $\phi_I(\xi)$ are the bivariate NURBS functions of order p and q in ξ and η directions, respectively.

2.2 Governing equations for a SLGS

As schematically illustrated in Fig. 2, a SLGS (uniform thickness *h*) is considered along with the cartesian coordinate system. The transverse displacement of the defected SLGS is expressed with *w*.

Employing the classical laminated plate (Kirchhoff) assumption, the displacement parts (u_x,u_y,u_z) for an optional point can be presented as (Liu 2003)

$$u_x=-z\frac{\partial w(x,y,t)}{\partial x},u_y=-z\frac{\partial w(x,y,t)}{\partial y},u_z=w(x,y,t)$$
$$\{u_x,u_y,u_z\}=\left\{-z\frac{\partial}{\partial x}\quad -z\frac{\partial}{\partial y}\quad 1\right\}^T w=Tw \tag{12}$$

Utilizing Eq. (12), the linear strain components are denoted as

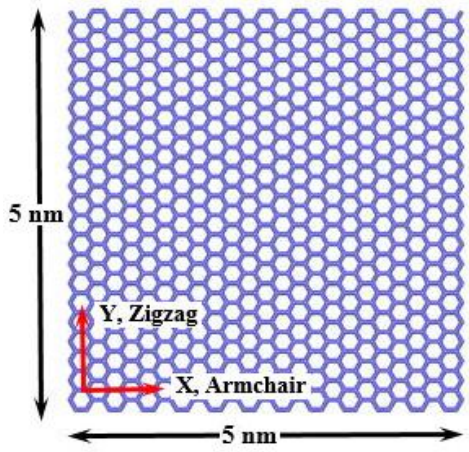

Fig. 2 The Schematic of a SLGS

$$\varepsilon_{xx}=-z\frac{\partial^2 w}{\partial x^2},\ \varepsilon_{yy}=-z\frac{\partial^2 w}{\partial y^2},\gamma_{xy}=-2z\frac{\partial^2 w}{\partial x\partial y}$$
$$\left\{\varepsilon_{xx},\varepsilon_{yy},\gamma_{xy}\right\}=z\left\{-\frac{\partial^2}{\partial x^2}\ -\frac{\partial^2}{\partial y^2}\ -2\frac{\partial^2}{\partial x\partial y}\right\}^T w=\boldsymbol{L}w \tag{13}$$

In which ε_{xx} and ε_{yy} demonstrate the normal strain members, and the term γ_{xy} denotes the shear strain part. By taking into account the plane stress assumption and using the nonlocal constitutive equation of Eringen (1983), the nonlocal constitutive stress-strain relations for an orthotropic SLGS can be expressed as below

$$(1-\mu\nabla^2)\begin{Bmatrix}\sigma_{xx}^{nl}\\ \sigma_{yy}^{nl}\\ \sigma_{xy}^{nl}\end{Bmatrix}=\begin{bmatrix}\frac{E_1}{(1-\upsilon_{12}\upsilon_{21})} & \frac{\upsilon_{12}E_2}{(1-\upsilon_{12}\upsilon_{21})} & 0\\ \frac{\upsilon_{12}E_2}{(1-\upsilon_{12}\upsilon_{21})} & \frac{E_2}{(1-\upsilon_{12}\upsilon_{21})} & 0\\ 0 & 0 & G_{12}\end{bmatrix}\begin{Bmatrix}\varepsilon_{xx}\\ \varepsilon_{yy}\\ \gamma_{xy}\end{Bmatrix} \tag{14}$$

Where E_1 and E_2 are, respectively, the Young's moduli in orientations 1 and 2. Also, G_{12} refers to the shear modulus, and Poisson's ratios are presented with ϑ_{12} and ϑ_{21}. Furthermore, the symbol $\mu=(e_0 a)^2$ is the nonlocal term, which is able to consider the small scale effect into the governing equations of the motion. However, e_0 refers to the calibration coefficients, which can be determined from experiment or the results of MD simulation. It should be noted that here, a is the internal characteristic length and $\nabla^2=\frac{\partial^2}{\partial x^2}+\frac{\partial^2}{\partial y^2}$ demonstrates the two-dimensional Laplacian operator. Applying the linear strain components of Eq. (13) and the nonlocal constitutive stress-strain relations of Eq. (14), the stress resultants in terms of transverse deflection of an orthotropic SLGS can be written as (Hosseini Hashemi *et al*. 2015)

$$M_{xx}\left(1-\mu\nabla^2\right)=-D_{11}\frac{\partial^2 w}{\partial x^2}-D_{12}\frac{\partial^2 w}{\partial y^2},$$
$$M_{yy}\left(1-\mu\nabla^2\right)=-D_{22}\frac{\partial^2 w}{\partial y^2}-D_{12}\frac{\partial^2 w}{\partial x^2}, \tag{15}$$
$$M_{xy}\left(1-\mu\nabla^2\right)=-2D_{66}\frac{\partial^2 w}{\partial x\partial y}$$

where

$$(M_{xx},M_{yy},M_{xy})=\int_{-\frac{h}{2}}^{\frac{h}{2}}\left(\sigma_{xx}^{nl},\sigma_{yy}^{nl},\sigma_{xy}^{nl}\right)zdz \tag{16}$$

$$D_{11}=\frac{E_1h^3}{12(1-\upsilon_{21}\upsilon_{12})},D_{12}=\frac{\upsilon_{12}E_2h^3}{12(1-\upsilon_{21}\upsilon_{12})}$$
$$D_{22}=\frac{E_2h^3}{12(1-\upsilon_{21}\upsilon_{12})},D_{66}=\frac{G_{12}h^3}{12} \tag{17}$$

It is noteworthy that for free vibration problem, the matrix-vector expressions of the strain energy Π_U and kinetic energy Π_T can be defined as

$$\Pi_U=\frac{1}{2}\int_V\varepsilon^T\sigma dV,\Pi_T=\frac{1}{2}\int_V\rho\dot{u}^T\dot{u}dV \tag{18}$$

Where V stands for the volume of orthotropic SLGS. Now, Hamilton's variational principle is used to achieve the governing differential equations of motion equation (Norouzzadeh and Ansari, 2018)

$$\delta\int_{t_1}^{t_2}(\Pi_T-\Pi_U)dt=0 \tag{19}$$

By substituting the deflection w from Eq. (10), the final undamped dynamic discrete equations for free vibration analysis in the present isogeometric method can be derived as

$$M\ddot{w}+Kw=0 \tag{20}$$

where w and $\ddot{w}$ are the vectors of the deflection and acceleration at the control points. K and M, respectively, stand for global stiffness and mass matrices which are defined as

$$K_{IJ}=\int_A B_I^T D B_J dA \tag{21}$$

$$M_{IJ}=\int_A\begin{Bmatrix}(\frac{\rho h^3}{12})(\frac{\partial\phi_I}{\partial x}\frac{\partial\phi_J}{\partial x}+\frac{\partial\phi_I}{\partial y}\frac{\partial\phi_J}{\partial y})+\\ \rho h\phi_I(1-\mu\nabla^2)\phi_J\end{Bmatrix}dA \tag{22}$$

$$B_I=\left\{-\frac{\partial^2\phi_I}{\partial x^2}\ -\frac{\partial^2\phi_I}{\partial y^2}\ -2\frac{\partial^2\phi_I}{\partial x\partial y}\right\}^T \tag{23}$$

In the above-mentioned equations, ρ and h are the density and thickness of the plate, respectively. A general solution for the homogenous equation given in Eq. (20) can be written as

$$w=\bar{w}e^{i\omega t} \tag{24}$$

Here i is the imaginary unit, ω indicates natural frequency, t represents time, and $\bar{w}$ is the eigenvector. By substituting Eq. (24) into Eq. (20), the natural frequency ω of the free vibration of the plate can be obtained by solving the following eigenvalue equation

$$(K-\omega^2M)\bar{w}=0 \tag{25}$$

2.3. Essential Boundary conditions

In this paper, we use a simple and efficient technique which was first proposed by Kiendl *et al*. (2009) for analysis of shell structures. In this technique, clamped boundary conditions can be imposed by simply fixing the deflection of the plate at the first two rows of control points from the desired boundary. This is based on the fact that the slopes at the boundary of a NURBS surface are defined by the first two rows of control points from this boundary (Kiendl *et al.* 2009). Simply supported boundary condition is also imposed by fixing the deflection of the first row of control points from the boundary.

3. Numerical simulations

3.1 Validation and comparison study for isogeometric approach

Table 1 Comparison study of the non-dimensional natural frequencies of completely free isotropic square plate

Mode	Present method (12*12)	Liu and Chen (2001)	Analytical solution (Abbassian *et al*. 1987)	FEM (Abbassian *et al.* 1987)	
				HOE	LOE
4	3.670	3.670	3.670	3.567	3.682
5	4.427	4.429	4.427	4.423	4.466
6	4.927	4.930	4.926	4.875	4.997
7	5.900	5.901	5.929	5.851	5.942
8	5.900	5.901	5.929	5.851	5.942
9	7.818	7.832	7.848	7.820	8.079

Table 2 Comparison study of the non-dimensional natural frequencies of simply supported isotropic square plate

Mode	Present method (12*12)	Analytical solutions (Abbassian *et al.* 1987)	Liu and Chen (2001)	
			Regular nodes	Irregular nodes
1	4.443	4.443	4.443	4.453
2	7.025	7.025	7.031	7.033
3	7.025	7.025	7.036	7.120
4	8.886	8.886	8.892	8.912
5	9.938	9.935	9.959	9.966
6	9.938	9.935	9.966	10.010
7	11.329	11.327	11.341	11.345
8	11.329	11.327	11.341	11.540
9	12.971	-	13.032	12.994
10	12.971	-	13.036	13.064

Table 3 Comparison study of the non-dimensional natural frequencies of fully clamped isotropic square plate

Mode	Present method (12*12)	Analytical solutions (Abbassian *et al.* 1987)	Liu and Chen (2001)	
			Regular nodes	Irregular nodes
1	5.999	5.999	6.017	5.999
2	8.568	8.568	8.606	8.596
3	8.568	8.568	8.606	8.602
4	10.401	10.407	10.439	10.421
5	11.469	11.472	11.533	11.507
6	11.496	11.498	11.562	11.528
7	12.829	-	12.893	12.925
8	12.829	-	12.896	12.986
9	14.468	-	14.605	14.570
10	14.468	-	14.606	14.604

To show the correctness and validity of the achieved formulation, several numerical examples with different boundary conditions are investigated in this section. The obtained results of present isogeometric approach are verified by comparing with other numerical or analytical solutions available in the literature. Firstly, Natural frequencies of an isotropic square plate without considering nonlocal term, and three types of boundary condition including Free (F), Simply supported (S) and Clamped (C) are investigated. The natural frequencies of a free square plate are listed in Table 1. It is observed that the calculated results are in good agreement with the results of other research works. In this table, HOE denotes eight-nodes semi-loof thin shell element (4*4 mesh); LOE denotes four-noded iso-parametric shell element (8*8 mesh). The first three frequencies corresponding to the rigid displacements are zero and are not reported. Natural frequencies of a simply supported and fully clamped square plates are computed using the present method. The results are shown in Tables 2 and 3, from these tables, one can find that

Table 4 Non-dimensional natural frequency of fully simply supported isotropic square nanoplate

a/h	μ (nm^2)	Present method	Norouzzadeh and Ansari (2018)	Nguyen et al. (2015) RPT	Nguyen et al. (2015) Quasi-3D	Aghababaei and Reddy (2009) TSDT	Aghababaei and Reddy (2009) FSDT	Aghababaei and Reddy (2009) CPT
10	0	0.0955	0.0931	0.0930	0.0920	0.0935	0.0930	0.0963
	1	0.0874	0.0850	0.0850	0.0841	0.0854	0.0850	0.0880
	2	0.0811	0.0788	0.0788	0.0779	0.0791	0.0788	0.0816
	3	0.0759	0.0738	0.0737	0.0729	0.0741	0.0737	0.0763
	4	0.0717	0.0696	0.0695	0.0688	0.0699	0.0696	0.0720
20	0	0.0240	0.0239	0.0239	0.0239	0.0239	0.0239	0.0241
	1	0.0219	0.0218	0.0218	0.0218	0.0218	0.0218	0.0220
	2	0.0203	0.0202	0.0202	0.0202	0.0202	0.0202	0.0204
	3	0.0190	0.0189	0.0189	0.0189	0.0189	0.0189	0.0191
	4	0.0179	0.0178	0.0178	0.0178	0.0179	0.0178	0.0180

present results are in good agreement with those of the other solutions.

To testify the validity of the present method, a comparison between the fundamental natural frequency obtained for an isotropic square nanoplate against different values of the nonlocal parameters with those obtained by other researchers (Norouzzadeh and Ansari 2018, Nguyen *et al.* 2015, Aghababaei and Reddy 2009) is indicated in Table 4. By briefly reviewing the computed results in this table, the accuracy of present formulations is determined.

3.2. Molecular dynamic approach

3.2.1 MD Simulation of pristine and defected single layer graphene sheets

All simulations are carried out with open source well-known software i.e., large-scale atomic/molecular massively parallel simulator (LAMMPS) package, using adaptive intermolecular reactive bond order (AIREBO) potential which is a suitable potential function for simulation of C-C bonding interaction (Stuart *et al.* 2008, Plimpton 1995).

Before applying strain, the sample is relaxed over 25 ps and the time step is selected to be 0.5 fs. The isothermal-isobaric (NPT) and isothermal-isovolumetric (NVT) ensembles are used for the simulation. Since the present continuum model does not consider thermal effects, all MD simulations are performed at low temperature conditions, i.e., 2 K. After the graphene sample has reached equilibrium, the strain is applied to the sample along the x- and y-direction at a rate of 0.001 ps (Fig. 2) and virial stress is used as a measure of mechanical stress of the graphene sheets (Tsai 1979, Zhou 2003, Subramaniyan *et al*. 2008).

3.2.2 Validation of MD approach for defect-free single layer graphene sheet

Recently mechanical properties of graphene sheet have been investigated both experimentally and theoretically (Ansari *et al*. 2012, Lee *et al.* 2008). Before discussion on obtained results from simulation, for validation of numerical model and computer simulation code first we compare the results obtained from simulation of a mono layer graphene with theoretical and experimental results of other papers. Fig. 3 illustrates schematic of a graphene sheet under tension loading in two directions: (a) armchair and (b) zigzag. Fig. 4 depicts stress-strain curve for graphene sheet under tension loading in both armchair and zigzag directions. The Young's and shear modulus can be estimated from a linear portion of the stress-strain curve from zero to 0.02 strain. The simulated Young's modulus in the first strain is 906.09 and 965.73 TPa for zigzag and armchair graphene sheet, respectively. This is also in good agreement with the experimental results of 1.0 TPa (Lee *et al.* 2008). However, the reported Young's modulus in the literature has a wide range of dispersion ranging from 0.5 to 1.4 TPa as shown in Table 5.

The value of shear modulus (G_{xy}) is 306.51 GPa. It shows that shear modulus of pristine graphene is high compared to other common materials as well as its tensile properties. In order to validate our results we have found that our predicted shear modulus of graphene is in good agreement with experimental value of 280 GPa and simulation value of 280 GPa which have been recently reported (Liu *et al.* 2012, Min and Aluru 2011).

3.2.3 Effect of vacancy defect type and degree on mechanical properties of graphene sheets

The simulated pristine graphene consists of 1008 carbon atoms with a size of 5 nm*5 nm with periodic boundary conditions applied along two planar x and y directions (Fig. 2).

In our study, the effects of several usual defects, SV or DV defects, on Young's and shear modulus are investigated. The SV and DV defects are respectively created by removing one carbon atom and two adjacent atoms on the pristine graphene sheet, as shown in Fig. 5.

Figs. 6 and 7 show the effect of different types and degree of defects on the Young's modulus of graphene sheets. Here the defect degree of vacancies considered as the number of removed atoms to the total number of atoms for the pristine graphene. According to the Table 6 with the increasing of defect degree the amount of shear modulus decreasing. It is observed that both kinds of defects decrease the Young's and shear modulus of graphene and

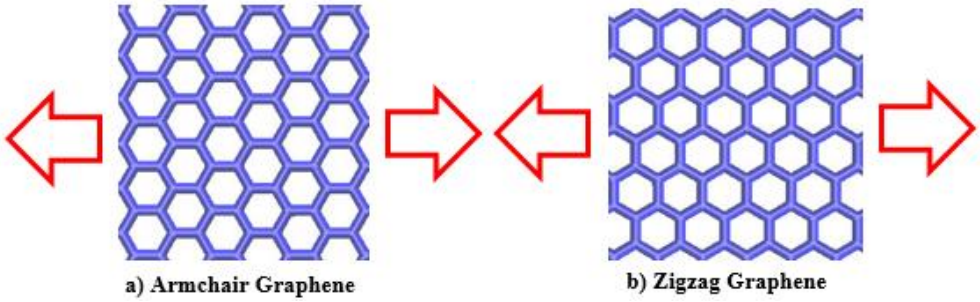

Fig. 3 Single graphene sheet under tension loading in: (a) Armchair direction and (b) Zigzag direction

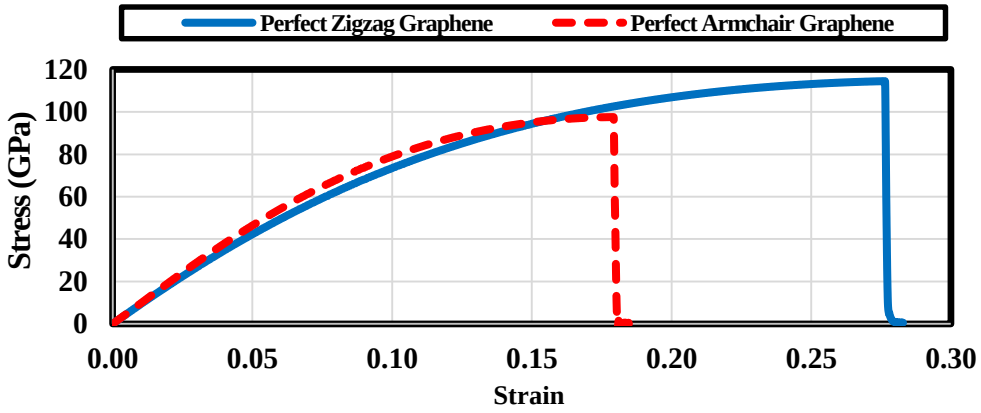

Fig. 4 The Stress-Strain curves of pristine graphene sheet with tensile loading applied in armchair and zigzag directions

Table 5 A comparison of the computed mechanical properties in the present study and the ones reported in the literature

Study	Method	Young's modulus (TPa)
Present	Molecular Dynamic	0.965
Lee *et al*. (2008)	Experimental	1± 0.1
Jiang *et al*. (2009)	Molecular Dynamic	1.1
Shen *et al.* (2010)	Molecular Dynamic	0.905
Ni *et al.* (2010)	Molecular Dynamic	1.13
Tsai and Tu (2010)	Molecular Dynamic	0.912
Kvashnin *et al*. (2010)	Molecular Mechanics	1.39 (average)
Reddy *et al.* (2006)	Continuum mechanics	0.669
Liu *et al.* (2007)	Density Functional Theory	1.05
Sakhaee-Pour (2009)	Finite Element	1.025
Georgantzinos *et al*. (2010)	Finite Element	1.367
Neek-Amal and Peteers (2010)	Molecular Dynamic	0.501 ±0.032
Yanovsky *et al*. (2009)	Quantum mechanics	0.737

the detrimental effect increases with the increasing of defects degree, but the degree of the detrimental effects differ with defect type. The Young's and shear modulus of a graphene with SV defects are much smaller than graphene with DV defects.

Figs. 8-11 show the influence of different vacancy types and degrees on the stress-strain curve of a 5*5 nm perfect and defected graphene. These figures show that vacancies greatly reduce the tensile strength and fracture strain for both zigzag and armchair graphene sheets. Figs. 12(a)-12(c) shows the influence of different vacancy types and degrees

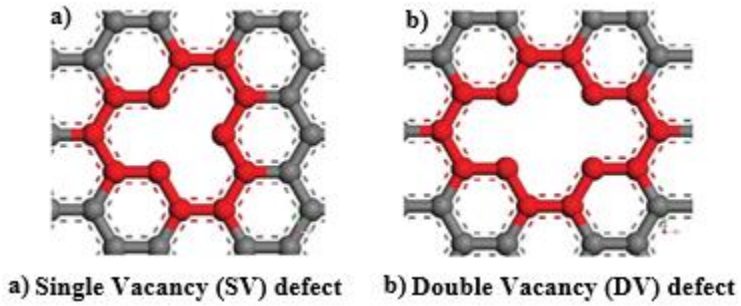

Fig. 5 Vacancy defects in single layer graphene sheets

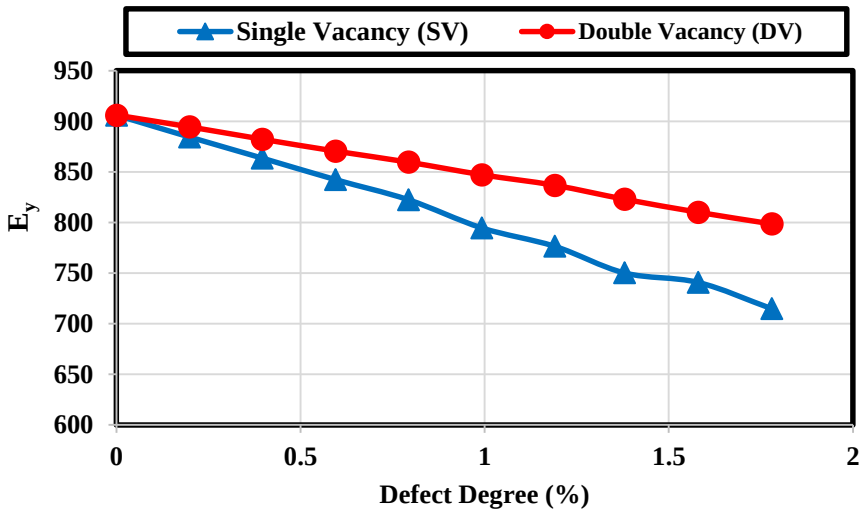

Fig. 6 The influence of defect degree on the E_y of single layer graphene sheet

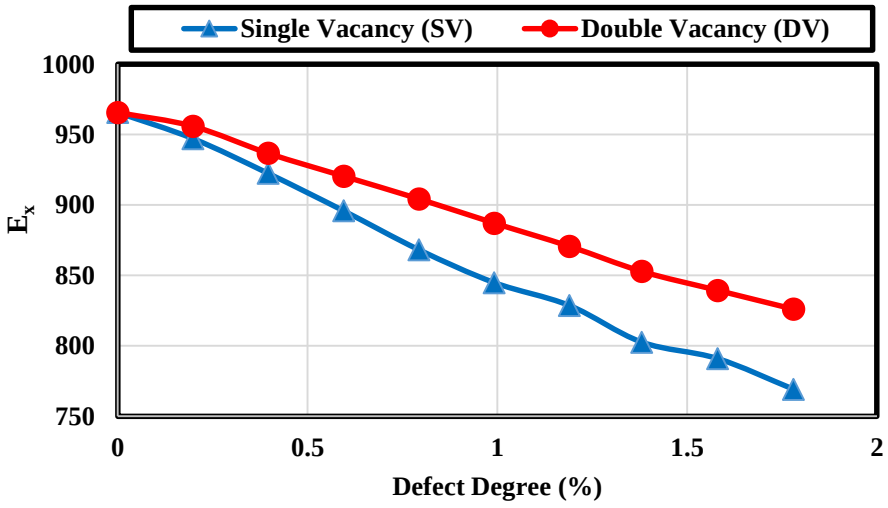

Fig. 7 The influence of defect degree on the E_x of single layer graphene sheet

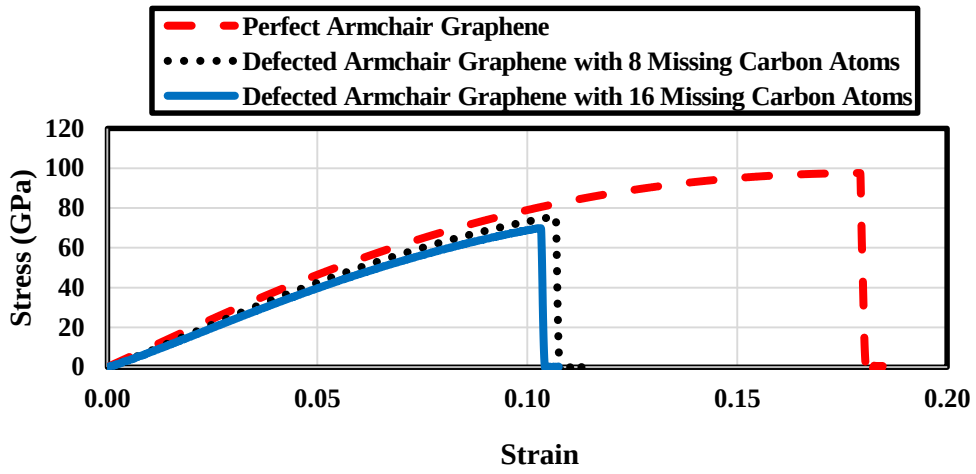

Fig. 8 The Stress-Strain curves of perfect and SV defected Armchair graphene sheet

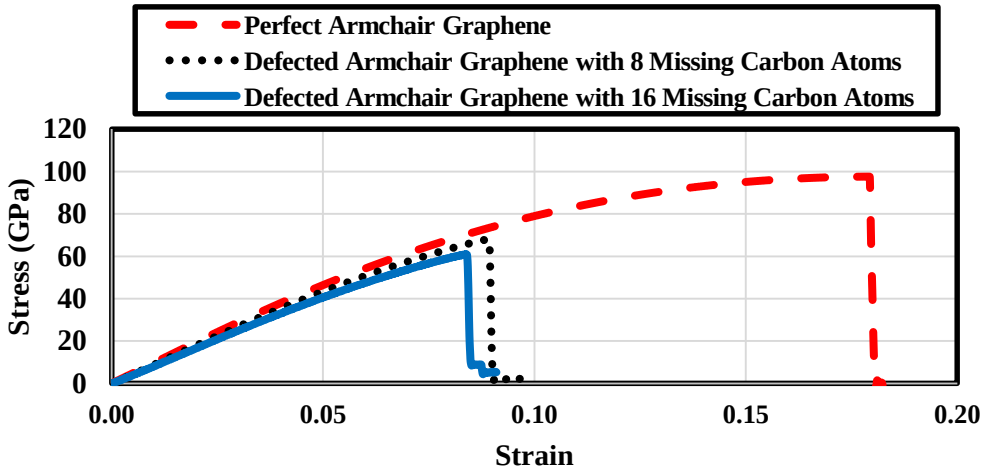

Fig. 9 The Stress-Strain curves of perfect and DV defected Armchair graphene sheet

Table 6 The effect of defect degree of Single and Double vacancy defects on the shear modulus

Defect degree (%)	G_{xy} (GPa) for SV defect	G_{xy} (GPa) for DV defect
0	306.51	306.51
0.198	276.07	291.54
0.396	246.81	269.48
0.595	240.47	262.91
0.793	221.15	251.49
0.992	186.56	239.52
1.190	182.27	237.16
1.38	179.96	220.52
1.58	178.17	215.12
1.78	156.29	204.43

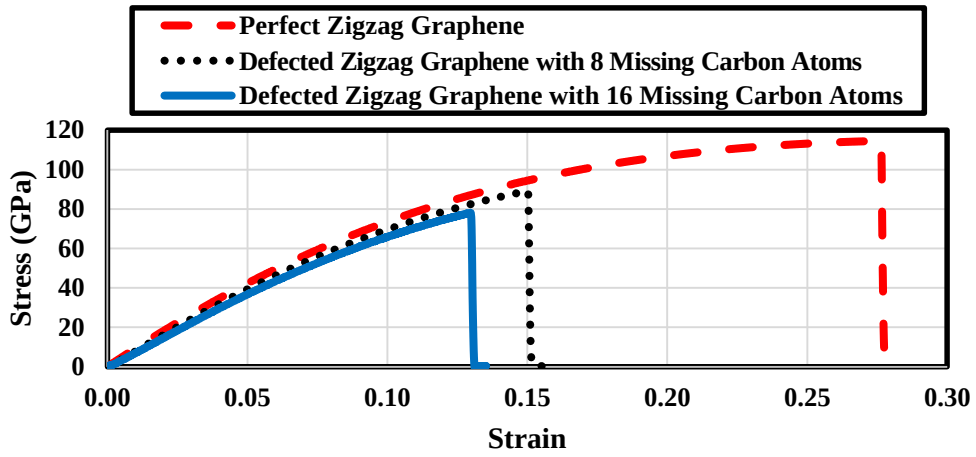

Fig. 10 The Stress-Strain curves of perfect and SV defected Zigzag graphene sheet

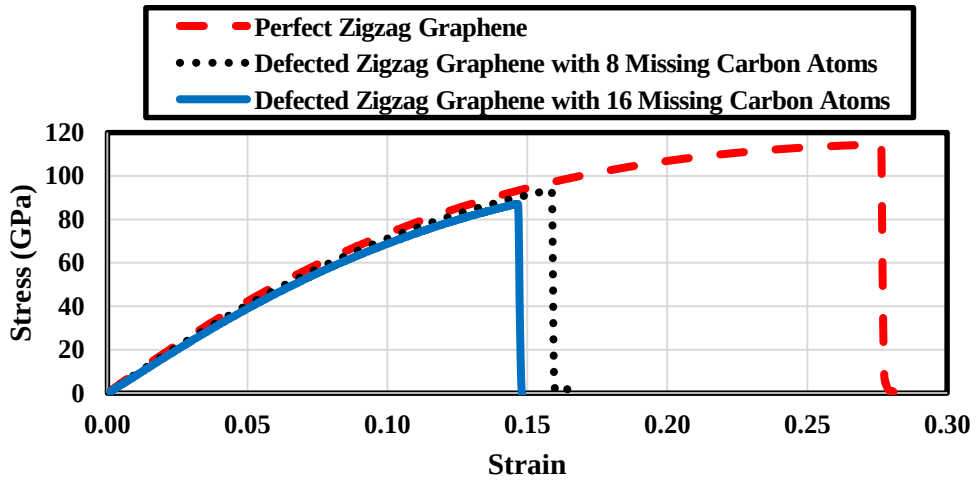

Fig. 11 The Stress-Strain curves of perfect and DV defected Zigzag graphene sheet

on the fracture stage of a 5*5 nm perfect and defected graphene. It is crystal clear that the vacancies have a big effect on the shape of fractures.

4. Benchmark results

Numerical computations are carried out in this section to better understand the impact of various parameters (nonlocal, mode number and boundary conditions) and DV and SV defects on the variation of the system natural frequency. In this study, we consider a graphene sheet with a size of 5*5 (nm). The mechanical properties of defected graphene for different defect degree have been estimated in the previous sections using molecular dynamic approach.

The density and effective thickness of the graphene are assumed to be 2250 kg/m^3 and 0.34 nm; respectively. According to the results reported in section 3.1, considering 144 control points can lead to good results and convergence so other results are further calculated with this number of control points.

The influence of missing carbon atoms number for both defect types including single and double vacancy defects is investigated in Figs. 13 and 14. These figures show that with increasing the number of missing carbons, the natural frequency of graphene decreases. Also, because of the softening effect of nonlocal term on the system, the natural frequency decreases by increasing nonlocal parameter. It is observed that the discrepancy between the branches decreases for high amount of nonlocal parameter. It should be noted this tendency has been seen in other mode

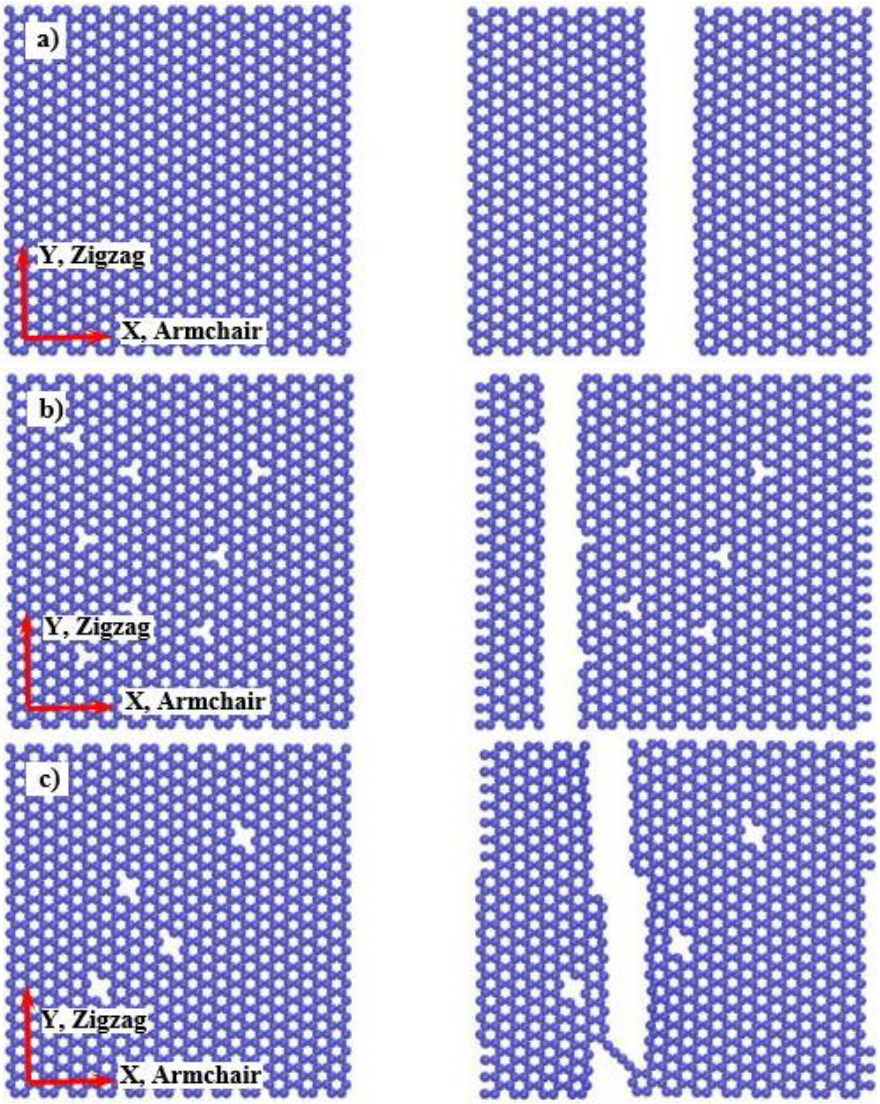

Fig. 12 Fracture of graphene sheets for different types and defect degrees; (a) perfect graphene, (b) SV defected graphene with 8 missing carbon atoms and (c) DV defected graphene with 8 missing carbon atoms.

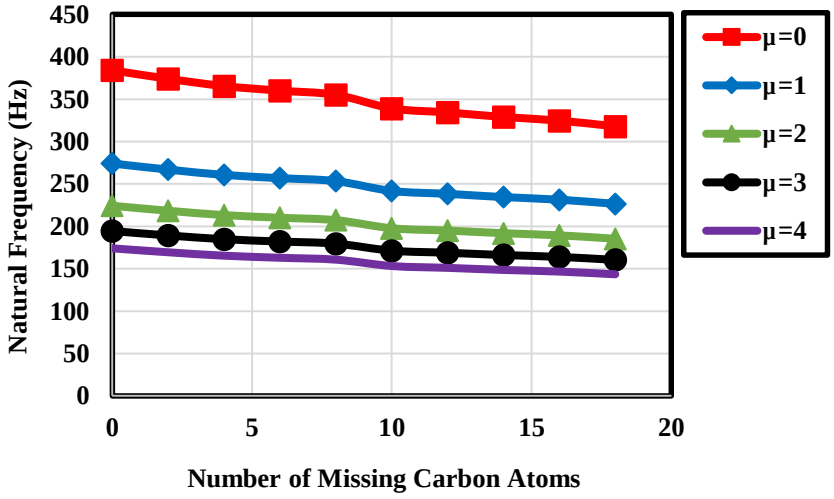

Fig. 13 The influence of missing carbon atoms number on the first natural frequency for completely clamped square graphene with Single Vacancy (SV) defects

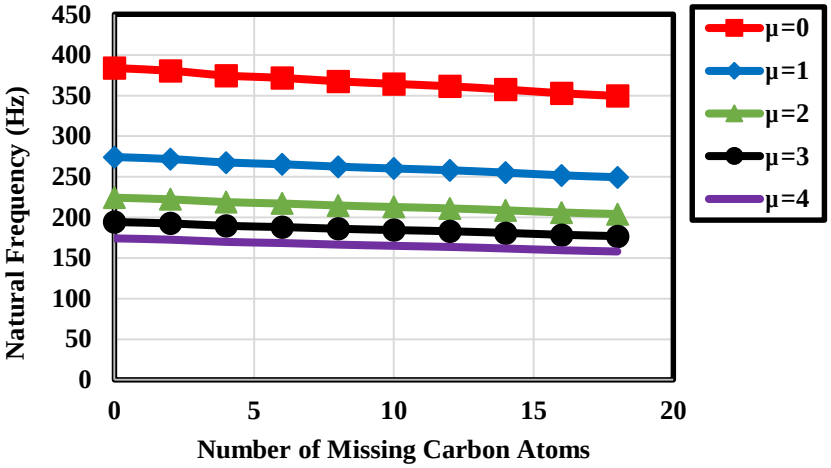

Fig. 14 The influence of missing carbon atoms number on the first natural frequency for completely clamped square graphene with Double Vacancy (DV) defects

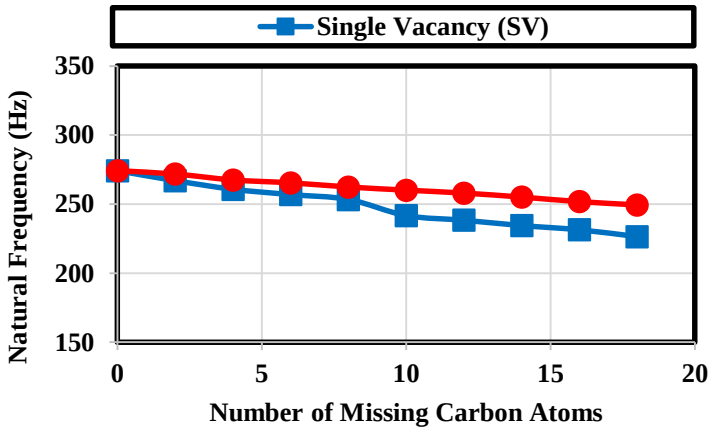

Fig. 15 The influence of Single and Double vacancy defects on the first natural frequency of fully clamped graphene for μ=1

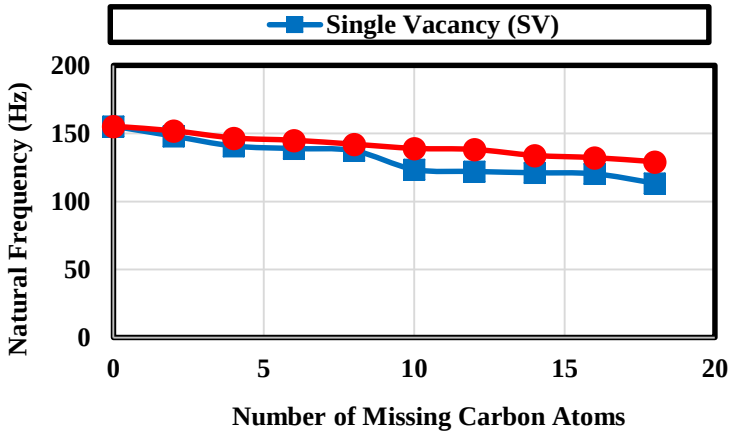

Fig. 16 The influence of Single and Double vacancy defects on the first natural frequency of fully simply supported graphene for μ=1

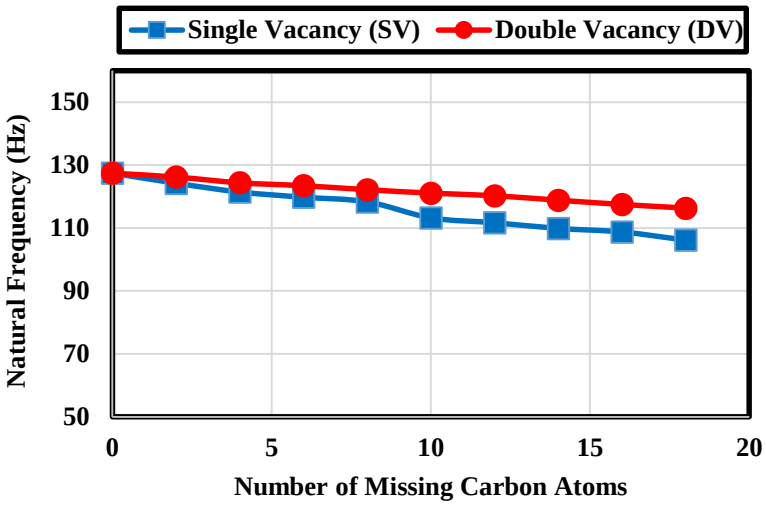

Fig. 17 The influence of Single and Double vacancy defects on the first natural frequency of completely free graphene for μ=1

numbers and boundary conditions but for the sake of brevity, they are not reported here.

Figs. 15-17, show the effect of single and double vacancy defects on the natural frequency of graphene with different boundary conditions. These figures reveal that Single Vacancy (SV) clusters cause more reduction in the natural frequencies of SLGS than Double Vacancy (DV) clusters. The same trend has been seen for other mode numbers.

5. Conclusions

This paper deals with vibration analysis of vacancy defected graphene sheet as a nonisotropic structure using molecular dynamic and continuum approaches. The influence of structural defects on the vibration of graphene sheets is considered by applying the mechanical properties of defected graphene sheets. Molecular dynamic simulations have been performed to estimate the mechanical properties of graphene with single- and double-vacancy defects using open source software i.e., large-scale atomic/molecular massively parallel simulator (LAMMPS). The correctness of the obtained results is checked via comparing with existing data in the literature and good agreement is eventuated. As a result, the effectiveness and the accuracy of the present IGA approach have been demonstrated and it is shown that the IGA is efficient, robust and accurate in terms of nanoplate problems. From this study some conclusions can be made as following:

- It is observed that both kinds of defects (SV and DV) decrease the Young's and shear modulus of graphene and the detrimental effect increases with the increasing of defects degree.
- The degree of the detrimental effects differ with defect type. The Young's and shear modulus of the graphene with SV defects are much smaller than graphene with DV defects.
- According to the results, with the increasing of defect degree the amount of shear modulus decreasing.
- It is observed that SLGSs with all types of defects have lower natural frequencies compared to perfect SLGSs.
- Single Vacancy (SV) clusters cause more reduction in natural frequencies of SLGSs than Double Vacancy (DV) clusters.
- Results indicate that because of the softening effect of nonlocal parameter, the natural frequency decreases with increasing this parameter.

References

Abbassian, F., Dawswell, D.J. and Knowles, N.C. (1987), "Free Vibration Benchmarks. Atkins Engineering Sciences": Glasgow.

Aghababaei, R. and Reddy, J.N. (2009), "Nonlocal third-order shear deformation plate theory with application to bending and vibration of plates", *J. Sound Vib.*, **326**(1-2), 277-289. https://doi.org/10.1016/j.jsv.2009.04.044.

Ahmed Houari, M.S., Bessaim, A., Bernard, F., Tounsi, A. and Mahmoud, S.R. (2018), "Buckling analysis of new quasi-3D FG nanobeams based on nonlocal strain gradient elasticity theory and variable length scale parameter", *Steel Compos. Struct.*, **28**(1), 13-24. https://doi.org/10.12989/scs.2018.28.1.013.

Ali, G.A.M., Makhlouf, S.A., Yusoff, M.M. and Chong, K.F. (2015), "Structural and electrochemical characteristics of graphene nanosheets as supercapacitor electrodes", *Rev. Adv. Mater. Sci.*, **41**(1), 35-43.

Ali, M.A., Mondal, K., Wang, Y., Jiang, H., Mahal, N.K., Castellano, M.J., Sharma, A. and Dong, L. (2017), "In situ integration of graphene foam–titanium nitride based bio-scaffolds and microfluidic structures for soil nutrient sensors",

Lab. Chip., **17**(2),274-285.

Al-Sherbini, A.S., Bakr, M., Ghoneim, I. and Saad, M. (2017), "Exfoliation of graphene sheets via high energy wet milling of graphite in 2-ethylhexanol and kerosene", *J. Adv. Res*., **8**(3), 209-215. https://doi.org/10.1016/j.jare.2017.01.004.

Ansari, R., Ajori, S. and Motevalli, B. (2012), "Mechanical properties of defective single-layered graphene sheets via molecular dynamics simulation", *Superlattices Microstruct*., **51**(2), 274-289. https://doi.org/10.1016/j.spmi.2011.11.019.

Ansari, R., Sahmani, S. and Arash, B. (2010), "Nonlocal plate model for free vibrations of single-layered graphene sheets", *Phys. Lett. A*., **375**(1), 53-62. https://doi.org/10.1016/j.physleta.2010.10.028.

Aristodemo, M. (1985), "A high-continuity finite element model for two dimensional elastic problems", *Comput. Struct*., **21**(5), 987-993. https://doi.org/10.1016/0045-7949(85)90211-1.

Bilotta, A., Formica, G. and Turco, E. (2010), "Performance of a high-continuity finite element in three-dimensional elasticity", *Int. J. Numer. Method. Biomed. Eng*., **26**(9), 1155-1175. https://doi.org/10.1002/cnm.1201.

Bu, H., Chen, Y., Zou, M., Yi, H., Bi, K. and Ni, Z. (2009), "Atomistic simulations of mechanical properties of graphene nanoribbons", *Phys. Lett. A*, **373**(37), 3359-3362. https://doi.org/10.1016/j.physleta.2009.07.048.

Chen, C.Q., Shi, Y., Zhang, Y.S., Zhu, J. and Yan, Y.J. (2006), "Size Dependence of Young's Modulus in ZnO Nanowires", *Phys. Rev. Lett*., **96**(7).

Chu, L., Shi, J. and Souza de Cursi, E. (2018), "Vibration analysis of vacancy defected graphene sheets by monte carlo based finite element method", *Nanomaterials*, **8**(7), 489. https://doi.org/10.3390/nano8070489.

Compagnini, G., Giannazzo, F., Sonde, S., Raineri, V. and Rimini, E. (2009), "Ion irradiation and defect formation in single layer graphene", *Carbon*, **47**(14), 3201–3207. https://doi.org/10.1016/j.carbon.2009.07.033.

Dastjerdi, S., Lot, M. and Jabbarzadeh, M. (2016), "The effect of vacant defect on bending analysis of graphene sheets based on the Mindlin nonlocal elasticity theory", *Compos. Part B Eng*., **98**(1), 78-87. https://doi.org/10.1016/j.compositesb.2016.05.009.

Eringen, A.C. (1983), "On differential equations of nonlocal elasticity and solutions of screw dislocation and surface waves", *J. Appl. Phys.*, **54**, 4703-4710. https://doi.org/10.1063/1.332803.

Fadaee, M. (2016), "Buckling analysis of a defective annular graphene sheet in elastic medium", *Appl. Math. Model*, **40**(3), 1863-1872. https://doi.org/10.1016/j.apm.2015.09.029.

Georgantzinos, S.K., Giannopoulos, G.I. and Anifantis, N.K. (2010), "Numerical investigation of elastic mechanical properties of graphene structures", *Mater. Des*., **31**(10), 4646-4654. https://doi.org/10.1016/j.matdes.2010.05.036.

Guo, Y., Ruess, M. and Gürdal, Z. (2014), "A contact extended isogeometric layerwise approach for the buckling analysis of delaminated composites", *Compos. Struct*., **116**(1), 55-66. https://doi.org/10.1016/j.compstruct.2014.05.006.

Hosseini Hashemi, S., Mehrabani, H. and Ahmadi-Savadkoohi, A. (2015), "Exact solution for free vibration of coupled double viscoelastic graphene sheets by visco pasternak medium", *Compos. Part B-Eng*., **78**, 377-383. https://doi.org/10.1016/j.compositesb.2015.04.008.

Hosseini, S.M. and Zhang, C. (2018), "Elastodynamic and wave propagation analysis in a FG Graphene platelets-reinforced nanocomposite cylinder using a modified nonlinear micromechanical model", *Steel Compos. Struct*., **27**(3), 255-271. https://doi.org/10.12989/scs.2018.27.3.255.

Hughes, T.J.R., Cottrell, J.A. and Bazilevs, Y. (2005), "Isogeometric analysis: CAD, finite elements, NURBS, exact geometry and mesh refinement", *Comput. Method. Appl. M.*, **194**(39-41), 4135-4195. https://doi.org/10.1016/j.cma.2004.10.008.

Jalali, S.K., Jomehzadeh, E. and Pugno, N.M. (2016), "Influence of out-of-plane defects on vibration analysis of graphene: Molecular Dynamics and Non-local Elasticity approaches", *Superlattices Microstruct*., **91**, 331-344. https://doi.org/10.1016/j.spmi.2016.01.023.

Javani, R., Bidgoli, M.R. and Kolahchi, R. (2019), "Buckling analysis of plates reinforced by Graphene platelet based on Halpin-Tsai and Reddy theories", *Steel Compos. Struct*., **31**(4), 419-427. https://doi.org/10.12989/scs.2019.31.4.419.

Jiang, J.W., Wang, J.S. and Li, B. (2009), "Young's modulus of graphene: A molecular dynamics study", *Phys. Rev. B*, **80**(11), 113405-113408.

Kapoor, H. and Kapania, R. (2012), "Geometrically nonlinear NURBS isogeometric finite element analysis of laminated composite plates", *Compos. Struct*., **94**(12), 3434–3447. https://doi.org/10.1016/j.compstruct.2012.04.028.

Karami, B., Janghorban, M., Shahsavari, D. and Touns, A. (2018), "A size-dependent quasi-3D model for wave dispersion analysis of FG nanoplates", *Steel Compos. Struct.*, **28**(1), 99-110. https://doi.org/10.12989/scs.2018.28.1.099.

Karami, B., Janghorban, M. and Tounsi, A. (2017), "Effects of triaxial magnetic field on the anisotropic nanoplates", *Steel Compos. Struct.*, **25**(3), 361-374. https://doi.org/10.12989/scs.2017.25.3.361.

Karami, B., Janghorban, M. and Tounsi, A. (2018), "Nonlocal strain gradient 3D elasticity theory for anisotropic spherical nanoparticles", *Steel Compos. Struct.*, **27**(2), 201-216 . https://doi.org/10.12989/scs.2018.27.2.201.

Kiendl, J., Bletzinger, K. U., Linhard, J. and Wuchner, R. (2009), "Isogeometric shell analysis with Kirchhoff-Love elements", *Comput. Method Appl. M*., **198**(49-52), 3902-3914. https://doi.org/10.1016/j.cma.2009.08.013.

Kitipornchai, S., He, X. Q. and Liew, K. M. (2005), "Continuum model for the vibration of multilayered graphene sheets", *Phys. Rev. B*., **72**(7), 075443-Published 29 August 2005.

Kumar, D. and Srivastava, A. (2016), "Elastic properties of CNT- and Graphene-reinforced nanocomposites using RVE", *Steel Compos. Struct.*, **21**(5), 1085-1103. http://dx.doi.org/10.12989/scs.2016.21.5.1085.

Kuzhir, P., Volynets, N., Maksimenko, S., Kaplas, T. and Svirko, Y. (2013), "Multilayered graphene in Ka-band: Nanoscale coating for aerospace applications", *J. Nanosci. Nanotechnol*., **13**(8), 5864-5867. https://doi.org/10.1166/jnn.2013.7551.

Kvashnin, A.G., Sorokin, P.B., Kvashnin, D.G. (2010), "The Theoretical Study of Mechanical Properties of Graphene Membranes", *Fullerenes, Nanotubes, and Carbon Nanostructures*, **18**(4-6), 497-500.

Lam, D.C.C., Yang, F., Chong, A.C.M., Wang, J. and Tong, P. (2003), "Experiments and theory in strain gradient elasticity", *J. Mech. Phys. Solids*, **51**(8), 1477-1508. https://doi.org/10.1016/S0022-5096(03)00053-X.

Lee, C., Wei, X.D., Kysar, J.W. and Hone, J. (2008), "Measurement of the elastic properties and intrinsic strength of monolayer graphene", *Science*, **321**(5887), 385-388. DOI: 10.1126/science.1157996.

Le-Manh, T. and Lee, J. (2014), "Postbuckling of laminated composite plates using NURBS-based isogeometric analysis", *Compos. Struct*., **109**, 286-293. https://doi.org/10.1016/j.compstruct.2013.11.011.

Le-Manh, T., Luu-Anh, T. and Lee, J. (2016), "Isogeometric analysis for flexural behavior of composite plates considering large deformation with small rotations", *Mech. Adv. Mater. Struct*., **23**(3), 328-336. https://doi.org/10.1080/15376494.2014.981616.

Lim, C.W.W., Zhang, G. and Reddy, J.N. (2015), "A higher-order nonlocal elasticity and strain gradient theory and its applications in wave propagation", *J. Mech. Phys. Solids*, **78**,

298-313. https://doi.org/10.1016/j.jmps.2015.02.001.

Liu, G.R. and Chen, X.L. (2001), "A mesh-free method for static and free vibration analyses of thin plates of complicated shape", *J. Sound Vib*., **241**(5), 839-855. https://doi.org/10.1006/jsvi.2000.3330.

Liu, F., Ming, P. and Li, J. (2007), "Ab initio calculation of ideal strength and phonon instability of graphene under tension", *Phys. Rev. B*, **76**(6), 064120- 064127.

Liu, G.R. (2003), "Meshfree Methods: Moving Beyond the Finite Element Method", (CRC Press, USA).

Liu, X., Metcalf, T.H., Robinson, J.T., Houston, B.H. and Scarpa, F. (2012), "Shear modulus of monolayer graphene prepared by chemical vapor deposition", *Nano. Lett.*, **12**(2), 1013-1017. https://doi.org/10.1021/nl204196v.

Ma, J., Alfè, D., Michaelides, A. and Wang, E. (2009), "Stone-Wales defects in graphene and other planar sp 2 -bonded materials", *Phys. Rev. B*, **80**, 1-4.

Malagu, M., Benvenuti, E. and Simone, A. (2012), "A Finite element and b-spline methods for one-dimensional non-local elasticity", *Proceedings of the ECCOMAS 2012: 6th European Congress on computational methods in applied sciences and engineering, September 2012*, Vienna University of Technology, Vienna, Austria.

Marina, P.E., Ali, G.A.M., See, L.M., Teo, E.Y.L., Ng, E.P. and Chong, K.F. (2016), "In situ growth of redox-active iron-centered nanoparticles on graphene sheets for specific capacitance enhancement", *Arab. J. Chem.*, https://doi.org/10.1016/j.arabjc.2016.02.006.

Marin, M. (2008), "Weak Solutions in Elasticity of Dipolar Porous Materials", *Math. Probl. Eng*., **2008**, http://dx.doi.org/10.1155/2008/158908, 1-8.

Marin, M. (2016), "An approach of a heat-flux dependent theory for micropolar porous media", *Meccanica*, **51**(5), 1127-1133. https://doi.org/10.1007/s11012-015-0265-2.

Marin, M. and Baleanu, D. (2016), "On vibrations in thermoelasticity without energy dissipation for micropolar bodies", *Bound. Value Probl*., **2016**(1), 1-19. https://doi.org/10.1186/s13661-016-0620-9.

Martinez-Asencio, J. and Caturla, M.J. (2015), "Molecular dynamics simulations of defect production in graphene by carbon irradiation", *Nucl. Instruments Methods Phys. Res. Sect. B Beam Interact with Mater. Atoms*, **352**, 225–228. https://doi.org/10.1016/j.nimb.2014.12.010.

Min, K. and Aluru, N.R. (2011), "Mechanical properties of graphene under shear deformation", *Appl. Phys. Lett.*, **98**(1), 013113.

Mirakhory, M., Khatibi, M.M. and Sadeghzadeh, S. (2018), "Vibration analysis of defected and pristine triangular single-layer graphene nanosheets", *Curr. Appl. Phys*., **18**(11), 1327-1337. https://doi.org/10.1016/j.cap.2018.07.014.

Mirzaei, M. and Kiani, Y. (2017), "Isogeometric thermal buckling analysis of temperature dependent FG graphene reinforced laminated plates using NURBS formulation", *Compos. Struct*.., **180**, 606-616. https://doi.org/10.1016/j.compstruct.2017.08.057.

Moradi-Dastjerdi, R. and Behdinan, K. (2019), "Thermoelastic static and vibrational behaviors of nanocomposite thick cylinders reinforced with Graphene", *Steel Compos. Struct.*, **31**(5), 529-539. https://doi.org/10.12989/scs.2019.31.5.529.

Nguyen, N.T., Hui, D., Lee, J. and Nguyen-Xuan, H. (2015), "An efficient computational approach for size-dependent analysis of functionally graded nanoplates", *Comput. Method. Appl. M*., **297**, 191-218. https://doi.org/10.1016/j.cma.2015.07.021.

Neek-Amal, M., Peeters, F.M. (2010), "Linear reduction of stiffness and vibration frequencies in defected circular monolayer graphene", *Phys. Rev. B*, **81**(23), 235437.

Ni, Z., Bu, H., Zou, M., Yi, H., Bi, K. and Chen, Y. (2010), "Anisotropic mechanical properties of graphene sheets from molecular dynamics", *Physica B*, **405**(5), 1301-1306. https://doi.org/10.1016/j.physb.2009.11.071.

Norouzzadeh, A. and Ansari, R. (2018), "Isogeometric vibration analysis of functionally graded nanoplates with the consideration of nonlocal and surface effects", *Thin-Wall. Struct*., **127**, 354-372. https://doi.org/10.1016/j.tws.2017.11.040.

Piegl, L. and Tiller, W. (1997), "The NURBS Book", (Monographs in Visual Communication) (Springer-Verlag, New York).

Plimpton, S. (1995), "Fast parallel algorithms for short-range molecular dynamics", *J. Comput. Phys.*, **117**(1), 1-19. https://doi.org/10.1006/jcph.1995.1039.

Pradhan, S.C. and Kumar, A. (2010), "Vibration analysis of orthotropic graphene sheets using nonlocal elasticity theory and differential quadrature method", *Compos. Struct*., **93**(2), 774-779. https://doi.org/10.1016/j.compstruct.2010.08.004.

Rajasekaran, G., Narayanan, P. and Parashar, A. (2016), "Effect of point and line defects on mechanical and thermal properties of graphene", *Crit. Rev. Solid State Mater. Sci.*, **41**(1), 47-71.

Reddy, C.D., Rajendran, S. and Liew, K.M. (2006), "Equilibrium configuration and continuum elastic properties of finite sized graphene", *Nanotechnology*, **17**(3), 864-870.

Ribeiro, P. and Chuaqui, T.R.C. (2019), "Non-linear modes of vibration of single-layer non-local graphene sheets", *Int. J. Mech. Sci*., **150**, 727-743. https://doi.org/10.1016/j.ijmecsci.2018.10.068.

Roh, H.Y. and Cho, M. (2004), "The application of geometrically exact shell elements to B-spline surfaces", *Comput. Method Appl. M*., **193**(23-26), 2261-2299. https://doi.org/10.1016/j.cma.2004.01.019.

Rouhi, S., Ansari, R. (2012), "Atomistic finite element model for axial buckling and vibration analysis of single-layered graphene sheets", *Phys. E. Low-Dimensional Syst. Nanostructures*, **44**(4), 764-772. https://doi.org/10.1016/j.physe.2011.11.020.

Sadeghi, M. and Naghdabadi, R. (2010), "Nonlinear vibrational analysis of single-layer graphene sheets", *Nanotechnology*, **21**(10).

Sakhaee-Pour, A. (2009), "Elastic buckling of single-layered graphene sheet", *Comput. Mater.* Sci., **45**(2), 266–270. https://doi.org/10.1016/j.commatsci.2008.09.024.

Sakhaee-Pour A. (2009), "Elastic properties of single-layered graphene sheet", *Solid State Commun*., **149**(1-2), 91-95. https://doi.org/10.1016/j.ssc.2008.09.050.

Sakhaee-Pour, A., Ahmadian, M.T. and Naghdabadi, R. (2008), "Vibrational analysis of single-layered graphene sheets", *Nanotechnology*, **19**(8), 85702. doi:10.1088/0957-4484/19/8/085702

Shahsavari, D., Karami, B. and Li, L. (2018), "A high-order gradient model for wave propagation analysis of porous FG nanoplates", *Steel Compos. Struct.*, **29**(1), 53-66. https://doi.org/10.12989/scs.2018.29.1.053.

Shen, L., Shen, H.S. and Zhang, C.L. (2010), "Temperature-dependent elastic properties of single layer graphene sheets", *Mater. Des.*, **31**(9), 4445-4449. https://doi.org/10.1016/j.matdes.2010.04.016.

Siddique, J.A., Attia, N.F. and Geckeler, K.E. (2015), "Polymer nanoparticles as a tool for the exfoliation of graphene sheets", *Mater. Lett*., **158**(1), 186-189.

Sobhy, M. (2014), "Thermomechanical bending and free vibration of single-layered graphene sheets embedded in an elastic medium", *Phys. E. Low-Dimensional Syst. Nanostructures*, **56**, 400-409. https://doi.org/10.1016/j.physe.2013.10.017.

Soleimani A., Dastani, K., Hadi, A. and Naei, M.H. (2019), "Effect of out-of-plane defects on the postbuckling behavior of Graphene sheets based on nonlocal elasticity theory", *Steel Compos. Struct.*, **30**(6), 517-534. https://doi.org/10.12989/scs.2019.30.6.517.

Soleimani, A., Naei, M.H. and Mashhadi, M.M. (2017), "Buckling analysis of graphene sheets using nonlocal isogeometric finite element method for NEMS applications", *Microsyst. Technol*.,

23(7), 2859-2871. https://doi.org/10.1007/s00542-016-3098-6.
Song M, Kitipornchai S. and Yang, J. (2017), "Free and forced vibrations of functionally graded polymer composite plates reinforced with graphene nanoplatelets", *Compos. Struct*., **159**, 579-588. https://doi.org/10.1016/j.compstruct.2016.09.070.
Stan, G., Ciobanu, C.V., Parthangal, P.M. and Cook, R.F. (2007), "Diameter-Dependent Radial and Tangential Elastic Moduli of ZnO Nanowires", *Nano Lett.*, **7**(12), 3691-3697. https://doi.org/10.1021/nl071986e.
Stuart, S.J., Tutein, A.B. and Harrison, J.A. (2000), "A reactive potential for hydrocarbons with intermolecular interactions", *J. Chem. Phys*., **112**, 6472-6487. https://doi.org/10.1063/1.481208.
Subramaniyan, A.K. and Sun, C.T. (2008), "Continuum interpretation of virial stress in molecular simulations", *J. Solids Struct*., **45**(14-15), 4340-4346. https://doi.org/10.1016/j.ijsolstr.2008.03.016.
Sun, S., Wang, C., Chen, M. and Zheng, J. (2013), "A novel method to control atomic defects in graphene sheets by selective surface reactions", *Appl. Surf. Sci*., **283**, 566–570. https://doi.org/10.1016/j.apsusc.2013.06.146.
Sun, X.Y., Hu, H., Caob, C. and Xua, Y.J. (2015), "Anisotropic vacancy-defect-induced fracture strength loss of graphene", *RSC Adv*., **5**(2), 13623-13627.
Sun, X., Fu, Z. and Xia, M. (2014), "Effects of vacancy defect on the tensile behavior of graphene", *Theor. Appl. Mech. Lett*., **4**(5), 51002. https://doi.org/10.1063/2.1405102.
Tasis, D., Papagelis, K., Spiliopoulos, P. and Galiotis, C. (2013), "Efficient exfoliation of graphene sheets in binary solvents", *Mater. Lett*., **94**, 47-50.
Tahouneh, V., Naei, M.H. and Mosavi Mashhadi, M. (2018), "The effects of temperature and vacancy defect on the severity of the SLGS becoming anisotropic", *Steel Compos. Struct.*, **29**(5), 647-657. https://doi.org/10.12989/scs.2018.29.5.647.
Thai, C.H., Nguyen-Xuan, H., Nguyen-Thanh, N., Le, T.H., Nguyen-Thoi, T. and Rabczuk, T. (2012), "Static, free vibration, and buckling analysis of laminated composite Reissner-Mindlin plates using NURBS-based isogeometric approach", *Int. J. Numer. Method. Eng*., **91**(6), 571-603. https://doi.org/10.1002/nme.4282.
Tornabene, F., Bacciocchi, M., Fantuzzi, N. and Reddy, J.N. (2018), "Multiscale approach for three-phase CNT/Polymer/Fiber laminated nanocomposite structures", *Polymer Composites*, In Press, DOI: 10.1002/pc.24520.
Tornabene, F., Fantuzzi, N., Ubertini, F. and Viola, E. (2015), "Strong formulation finite element method based on differential quadrature: a survey", *Appl. Mech. Rev*., **67**(2), 1-55.
Tran, L.V., Lee, J., Nguyen-Van, H., Nguyen-Xuan, H. and Wahab, M.A. (2015), "Geometrically nonlinear isogeometric analysis of laminated composite plates based on higher-order shear deformation theory", *Int. J. Non-Linear Mech.*, **72**, 42–52. https://doi.org/10.1016/j.ijnonlinmec.2015.02.007.
Tran, L.V., Phung-Van, P., Lee, J., Wahab, M.A. and Nguyen-Xuan, H. (2016), "Isogeometric analysis for nonlinear thermomechanical stability of functionally graded plates", *Compos. Struct*., **140**, 655-667. https://doi.org/10.1016/j.compstruct.2016.01.001.
Tsai, D.H. (1979), "The virial theorem and stress calculation in molecular dynamics", *J. Chem. Phys*., **70**, 1375-1382. https://doi.org/10.1063/1.437577.
Tsai, J.L. and Tu, J.F. (2010), "Characterizing mechanical properties of graphite using molecular dynamics simulation", *Mater. Des*., **31**(1), 194-199. https://doi.org/10.1016/j.matdes.2009.06.032.
Udupa, A. and Martini, A. (2011), "Model predictions of shear strain-induced ridge defects in graphene", *Carbon*, **49**(11), 3571-3578. https://doi.org/10.1016/j.carbon.2011.04.057.
Wang, X., Zhu, X. and Hu, P. (2015), "Isogeometric finite element method for buckling analysis of generally laminated composite beams with different boundary conditions", *Int. J. Mech. Sci*., **104**, 190-199. https://doi.org/10.1016/j.ijmecsci.2015.10.008.
Wei, Y., Wang, B., Wu, J., Yang, R. and Dunn, M.L. (2012), "Bending rigidity and Gaussian bending stiffness of single-layered graphene", *Nano Lett*., **13**(1), 26-30. https://doi.org/10.1021/nl303168w.
Wenhu Wu, Y. D.,Yin, J., Xie, W., Zhang, W., Wu, B., Jiang, Y. and Zhang, P. (2015), "Effect of vacancy distribution on the relaxation properties of graphene : A molecular dynamics study", IET Micro. *Nano Lett*., **10**(12).
Xie, G., Shen, Y., Wei, X., Yang, L., Xiao, H., Zhong, J. and Zhang, G. (2014), "A bond-order theory on the phonon scattering by vacancies in two-dimensional materials", *Electron. Spintron. devices*, 1-23. https://doi.org/10.1038/srep05085.
Yang, F., Chong, A.C.M., Lam, D.C.C. and Tong, P. (2002), "Couple stress based strain gradient theory for elasticity", *Int. J. Solids Struct*., **39**(10), 2731-2743. https://doi.org/10.1016/S0020-7683(02)00152-X.
Yanovsky, Y.G., Nikitina, E.A., Karnet, Y.N., Nikitin, S.M. (2009), "Quantum mechanics study of the mechanism of deformation and fracture of graphene", *Phys. Mesomech*., **12**(5-6), 254-262. https://doi.org/10.1016/j.physme.2009.12.007.
Yu, T.T., Yin, S., Bui, T.Q. and Hirose, S. (2015), "A simple FSDT-based isogeometric analysis for geometrically nonlinear analysis of functionally graded plates", *Finite Elem. Anal. Des*., **96**, 1-10. https://doi.org/10.1016/j.finel.2014.11.003.
Zhang, Y., Chen, Y., Zhou, K. and Liu, C. (2009), "Improving gas sensing properties of graphene by introducing dopants and defects : a first-principles study", *Nanotechnology*, **20**(18).
Zhang, Y., Lei, Z.X., Zhang, L.W., Liew, K.M. and Yu, J.L. (2015), "Nonlocal continuum model for vibration of single-layered graphene sheets based on the element-free kp-Ritz method", *Eng. Anal. Bound. Elem*., **56**, 90-97. https://doi.org/10.1016/j.enganabound.2015.01.020.
Zhou, M. (2003), "A new look at the atomic level virial stress: on continuum-molecular system equivalence", *P. Roy. Soc. A-Math. Phy.*, **459**(2), 2347-2392. https://doi.org/10.1098/rspa.2003.1127.

CC